

Majorana zero modes, spontaneous Z_2^f symmetry breaking, and long range edge correlation in Kitaev chains: analytic solutions and density-matrix-renormalization-group study

Jian-Jian Miao,^{1,2} Hui-Ke Jin,^{1,2} Fu-Chun Zhang,^{1,2} and Yi Zhou^{1,2}

¹*Department of Physics, Zhejiang University, Hangzhou 310027, China*

²*Collaborative Innovation Center of Advanced Microstructures, Nanjing 210093, China*

(Dated: September 13, 2016)

We study Kitaev model in one-dimension with open boundary condition by using exact analytic methods for non-interacting system in the half filled limit as well as in the symmetric case of $\Delta = t$, and by using density-matrix-renormalization-group method for interacting system with nearest neighbor repulsion. We show explicitly that the emergence of Majorana zero mode is associated with the spontaneous symmetry broken of fermion number parity operator Z_2^f , which is +1 for even number of fermions and -1 for odd number of fermions. Our results are in support of recent proposal by Klassen and Wen¹, who proposed such spontaneous symmetry broken in systems with Majorana zero modes. We suggest and examine an edge correlation function of Majorana fermions to characterize the long range order in the topological superconducting states and study the phase diagram of the interacting Kitaev chain.

PACS numbers: 71.10.Fd, 71.10.Pm, 74.20.-z, 03.75.Lm

I. INTRODUCTION

Majorana² zero mode (MZM) has attracted a lot of attention in the recent years³⁻⁵, which may emerge as a novel excitation in some topological condensed matter systems. MZMs obey non-Abelian statistics and have potential application to build robust qubits against decoherence in quantum computation^{6,7}. The emergence of MZMs has been theoretically proposed in a number of condensed matter systems, including chiral p -wave superconductors^{8,9}, $\nu = 5/2$ fractional quantum Hall system¹⁰, the interface between a topological insulator and an s -wave superconductor¹¹, proximity-induced superconductor for spin-orbit coupled nanowires^{12,13}, spin-orbit coupled semiconductor with externally applied Zeeman field¹⁴⁻¹⁶, and ferromagnetic atoms in proximity to superconductors^{17,18}. There also exist various experimental efforts to realize and detect MZMs in these proposed systems¹⁹⁻²⁸.

Among these candidates, the one-dimensional (1D) systems are of special theoretical interest for possible generalization to interacting systems. The interaction may change properties drastically in 1D systems. The Fermi liquid description of the interacting Fermi gas usually works in 2D or 3D. However, it breaks down in 1D and the systems become Luttinger liquids. Fortunately, there have been a number of many-body techniques suitable to study various 1D problems²⁹, which make the generalization of the MZMs in 1D models accessible. On the other hand, the interaction will modify topological systems violently, e.g. the non-interacting classification of fermionic systems³⁰⁻³² will “collapse” and there exists a continuous path connecting trivial and topological phases in 1D³³.

Recently, Klassen and Wen¹ observed that these fermionic systems always have a fermion number parity symmetry Z_2^f , which is +1 in a system of even number of

fermions and -1 in a system of odd number of fermions. The fermion number parity is a good quantum number in a system whose Hamiltonian commutes with Z_2^f . They proposed that Z_2^f is spontaneously broken in topologically nontrivial phases, resulting in two-fold topological degeneracy^{34,35}. They also pointed out that a MZM will change Z_2^f , and suggested that the 1+1D fermionic topological order³⁶⁻³⁸ can be viewed as a spontaneous Z_2^f symmetry breaking order and may thus be studied by using Landau theory for phase transition. Furthermore, they argued that the Z_2^f symmetry property is robust against interaction. Klassen and Wen constructed an effective Hamiltonian to model a chain of magnetic dots on a substrate of fully gapped superconductor. They used mean-field theory and a nonlocal fermion number parity order parameter to illustrate their proposal.

Kitaev chain⁸ is a prototype of 1D systems possessing MZMs at the two edges. It will be interesting to examine the idea Klassen and Wen put forward by studying the Kitaev model. The non-interacting Kitaev model was initially solved in a ring with periodic boundary condition. The edge state was then proposed to exhibit MZM. The model has been generalized to interacting case with nearest neighboring repulsive interaction. The interacting Kitaev model does not have analytic solutions in general cases except for a set of specially tuned parameters^{39,40}. The model can also be studied by numerical methods⁴⁰⁻⁴². In general, interacting effects on MZMs have been investigated in various systems, e.g. nanowires⁴³⁻⁴⁷, multiband nanowires⁴⁸, helical liquids⁴⁹, two-leg ladders⁵⁰, Josephson junctions⁵¹ and Abrikosov vortex lattice⁵². The interplay of disorder and interaction has also been analyzed^{53,54}. The MZM is stable against weak perturbations including the interaction and disorder. However, the generic interaction effect remains an open question, although lots

of efforts have been made, which includes the exact solution⁵⁵, topological classification^{33,56}, entanglement entropy investigation⁵⁷, many-body MZM operator^{58,59}, super-symmetry approaches⁶⁰⁻⁶³ and parafermion edge zero mode⁶⁴⁻⁶⁸.

In this paper, we shall first study non-interacting Kitaev chain of length L with open boundary condition by using an analytic method, which is accessible at zero chemical potential or at a symmetric point of the pairing and the hopping amplitudes, $\Delta = t$. We show that the first excited state has an energy degenerate to the ground state with an energy difference exponentially small as $\exp(-L/l_0)$, and $Z_2^f = +1$ in the ground state and $Z_2^f = -1$ in the first excited state. In the thermodynamic limit $L \rightarrow \infty$, the two states are degenerate and the edge state is a mixed parity state of Z_2^f . We propose a correlation function of the two Majorana operators as long range order parameter to describe non-trivial topological state with edge MZMs and calculate the long range correlation function explicitly. We then study Kitaev model with neighboring site repulsion in open boundary condition by using density matrix renormalization group (DMRG) method. We show that the property of the Z_2^f symmetry and the qualitative feature of the long range correlation remain unchanged in the interacting systems provided that the system is in the topological non-trivial phase. The phase diagram in the interacting model will also be discussed.

This paper is organized as follows. In Section II, the model Hamiltonian and Z_2^f symmetries are presented and Majorana fermion representation is introduced. In Section III, we study non-interacting models by using analytic solutions. A single-particle correlation function is introduced and its edge component is used to describe the topological order. In Section IV, numerical DMRG analysis is carried out to study interacting systems. Section V is devoted to discussions.

II. MODEL

Without loss of generality, we consider a chain of spinless fermions with open boundary condition. The Hamiltonian of such an interacting Kitaev chain is

$$H = \sum_{j=1}^{L-1} \left[-t \left(c_j^\dagger c_{j+1} + h.c. \right) + U (2n_j - 1) (2n_{j+1} - 1) - \Delta \left(c_j^\dagger c_{j+1}^\dagger + h.c. \right) \right] - \mu \sum_{j=1}^L \left(n_j - \frac{1}{2} \right), \quad (1)$$

where $c_j (c_j^\dagger)$ is fermion annihilation (creation) operator on site j , $n_j = c_j^\dagger c_j$ is the fermion number operator, t is the hopping matrix element, and Δ is the p -wave superconducting pairing potential induced by the proximity effect, μ is the chemical potential controlling the electron density, and U is the nearest neighbor interaction. One

can always choose Δ real and non-negative by the global transformation $c_j \rightarrow e^{i\varphi} c_j$. Similarly, one can study the case of $t \geq 0$ and $\mu \geq 0$ only, since the parameter transformations $t \rightarrow -t$ and $\mu \rightarrow -\mu$ can be realized by the gauge transformation $c_j \rightarrow i(-1)^j c_j$ and particle-hole conjugation $c_j \rightarrow (-1)^j c_j^\dagger$ respectively. Note that all these transformations will keep other parameters unchanged. In this paper, we only consider repulsive nearest neighbor interaction with $U \geq 0$. When $U = 0$, this model will reduce to the usual (non-interacting) Kitaev chain⁸.

The Hamiltonian has the fermion number parity Z_2^f symmetry, which is defined as

$$Z_2^f = e^{i\pi \sum_j n_j} = (-1)^{\hat{N}}, \quad (2)$$

where $\hat{N} = \sum_j n_j$ is the total fermion number, and it is obvious that $(Z_2^f)^2 = 1$ and $[H, Z_2^f] = 0$. Z_2^f conserves in the whole parameter space. In the presence of the pairing potential Δ , the total fermion number is not conserved but only conserved modulo 2.

II.1. Majorana fermion representation

We shall use the Majorana fermion representation to investigate the interacting Kitaev chain. Following Katsura *et al.*³⁹, we split one complex fermion operator into two Majorana fermion operators

$$c_j = \frac{1}{2} (\lambda_j^1 + i\lambda_j^2), \quad (3a)$$

$$c_j^\dagger = \frac{1}{2} (\lambda_j^1 - i\lambda_j^2). \quad (3b)$$

The Majorana fermion operators are real

$$(\lambda_j^a)^\dagger = \lambda_j^a, \quad (4)$$

and satisfy the anticommutation relations

$$\{\lambda_j^a, \lambda_l^b\} = 2\delta_{ab}\delta_{jl}, \quad (5)$$

where $a, b = 1, 2$. In the Majorana fermion representation, the Hamiltonian of the interacting Kitaev chain becomes

$$H = \sum_{j=1}^{L-1} \left[-\frac{i}{2} (t + \Delta) \lambda_{j+1}^1 \lambda_j^2 - \frac{i}{2} (t - \Delta) \lambda_j^1 \lambda_{j+1}^2 - U \lambda_j^1 \lambda_j^2 \lambda_{j+1}^1 \lambda_{j+1}^2 \right] - \frac{i}{2} \mu \sum_{j=1}^L \lambda_j^1 \lambda_j^2. \quad (6)$$

III. NON-INTERACTING KITAEV CHAINS

In this section, we consider the non-interacting Kitaev chains with open boundary condition and discuss the relations among the topological degeneracy, the Majorana

zero mode, and the broken Z_2 symmetry. We shall use analytic method to exactly solve the two non-interacting cases with $\Delta = t$, $U = 0$ and $\mu = 0$, $U = 0$ by the singular value decomposition (SVD) in Majorana fermion representation.

III.1. Non-interacting chains with $\Delta = t$

In this case, the transition between the topological superconductor and the trivial superconductor can be studied by tuning the chemical potential μ . The non-interacting Hamiltonian H_μ is quadratic in λ_j^1 and λ_j^2 and is given by

$$\begin{aligned} H_\mu &= \frac{i}{2} \left[\sum_{j=1}^{L-1} -2t\lambda_{j+1}^1\lambda_j^2 - \sum_{j=1}^L \mu\lambda_j^1\lambda_j^2 \right] \\ &= \frac{i}{2} \sum_{j,l=1}^L \lambda_j^1 B_{jl} \lambda_l^2, \end{aligned} \quad (7)$$

where B is a $L \times L$ real matrix,

$$B = - \begin{pmatrix} \mu & 0 & & & \\ 2t & \mu & & & \\ & & \ddots & \ddots & \\ & & & 2t & \mu & 0 \\ & & & & 2t & \mu \end{pmatrix}. \quad (8)$$

With the help of SVD, $B = U\Lambda V^T$, where Λ is a real diagonal matrix, U and V are real orthogonal matrices, H_μ can be diagonalized as follows,

$$\begin{aligned} H_\mu &= \frac{i}{2} \sum_k \lambda_k^1 \Lambda_k \lambda_k^2 \\ &= \sum_k \Lambda_k \left(c_k^\dagger c_k - \frac{1}{2} \right), \end{aligned} \quad (9)$$

where $\Lambda_k \geq 0$ are singular values of the matrix B , $c_k = \frac{1}{2}(\lambda_k^1 + i\lambda_k^2)$ and $c_k^\dagger = \frac{1}{2}(\lambda_k^1 - i\lambda_k^2)$ are the complex fermion operators.

In the weak pairing region, $\mu < 2t$, we find that (See Appendix A for details) the smallest singular value Λ_k is nonzero given by

$$\Lambda_{k_0} = \left(\frac{2t}{\mu} - \frac{\mu}{2t} \right) \left(\frac{\mu}{2t} \right)^L, \quad (10)$$

and the corresponding matrix elements

$$U_{jk_0} = A_{k_0} \sinh v(L+1-j), \quad (11a)$$

$$V_{jk_0} = A_{k_0} \sinh vj, \quad (11b)$$

where $A_{k_0} = 2e^{-vL} (1 - e^{-2v})^{1/2}$ is the normalization factor, and v is a positive real number determined by Eq. (A12).

It is worth noting that a similar model has been solved by Katsura *et al.*³⁹ using SVD. In their case, the chemical potential is half of the bulk's value at edge, $\mu_1 = \mu_L = \mu/2$, resulting in $\Lambda_{k_0} = 0$.

III.1.1. Topological degeneracy and the edge mode

It is well known that there exist two topologically distinct phases in the non-interacting Kitaev chain model^{8,70,71}. For strong pairing $\mu > 2t$, the system is in the trivial superconducting state, while for weak pairing $\mu < 2t$, the system is in the topological superconducting state.

In the trivial superconducting state, the energy spectrum is gapped and the ground state is non-degenerate. However, in the topological superconductor, the energy gap between the ground state $|0\rangle$ and the first excited state $|1\rangle \equiv c_{k_0}^\dagger |0\rangle$ is Λ_{k_0} given in Eq. (10), approaches to zero with the exponential factor $e^{-L \ln(2t/\mu)}$ in the large L limit. Thus, the k_0 -mode is a *zero mode* and the topological superconductor has two-fold degenerate ground states in thermodynamic limit. In other words, it is a gapped system with two-fold topological degeneracy¹.

Now we shall check that the first excited state $|1\rangle$ is an edge mode. It is a single particle (hole) excited state. The particle and hole parts of the wavefunction read

$$\begin{aligned} \langle 0 | c_j | 1 \rangle &= \langle 0 | c_j c_{k_0}^\dagger | 0 \rangle = \frac{1}{2} (U_{jk_0} + V_{jk_0}) \\ &= \frac{A_{k_0}}{2} [\sinh v(L+1-j) + \sinh vj] \end{aligned} \quad (12a)$$

and

$$\begin{aligned} \langle 0 | c_j^\dagger | 1 \rangle &= \langle 0 | c_j^\dagger c_{k_0}^\dagger | 0 \rangle = \frac{1}{2} (U_{jk_0} - V_{jk_0}) \\ &= \frac{A_{k_0}}{2} [\sinh v(L+1-j) - \sinh vj] \end{aligned} \quad (12b)$$

respectively, where Eq. (11) and Eq. (A2) have been used in the derivation. It is easy to see that this zero mode has a complex wave vector $k_0 = \pi + iv$ and the wavefunction is well localized at edges with localization length v^{-1} as demonstrated in Fig. 1.

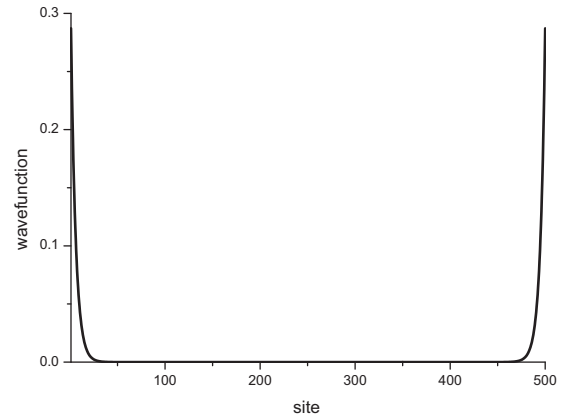


FIG. 1. The particle wavefunction $\langle 0 | c_j c_{k_0}^\dagger | 0 \rangle$ for the k_0 -mode with $L = 500$ and $v = 0.2$.

Now we would like to examine that the k_0 mode is indeed a Majorana mode, say, $c_{k_0}^\dagger = \pm c_{k_0}$, namely, it

coincides to its antiparticle. Using Eq. (A2), we have

$$c_{k_0}^\dagger = \frac{1}{2} (\lambda_{k_0}^1 - i\lambda_{k_0}^2) = \frac{1}{2} \sum_{j=1}^L (U_{jk_0} \lambda_j^1 - iV_{jk_0} \lambda_j^2). \quad (13)$$

By Eq. (11), we find that

$$c_{k_0}^\dagger = \begin{cases} c_{k_0}, & j \ll v^{-1}, \\ -c_{k_0}, & L+1-j \ll v^{-1}. \end{cases} \quad (14)$$

So that there exists one Majorana mode with $c_{k_0}^\dagger = c_{k_0}$ at the edge $j = 1$ and another Majorana mode with $c_{k_0}^\dagger = -c_{k_0}$ at the edge $j = L$.

III.1.2. Fermion number parity and edge correlation function

There are two characterizing features for topological ordered systems, (base-manifold dependent) ground state degeneracy and gapless edge states. Below we shall examine that the ground state degeneracy is associated with fermion number parity Z_2^f and propose an edge correlation function to describe the emerged edge states.

We note the ground state $|0\rangle$ and the excited state $|1\rangle$ have opposite fermion number parity

$$\langle 1 | Z_2^f | 1 \rangle = \langle 0 | c_{k_0} Z_2^f c_{k_0}^\dagger | 0 \rangle = -\langle 0 | Z_2^f | 0 \rangle. \quad (15)$$

In the thermodynamic limit, the first excited $|1\rangle$ is degenerate with the ground state $|0\rangle$. Then a generic ground state of the topological superconductor is a linear combination of these two states, $|GS\rangle = a|0\rangle + bc_{k_0}^\dagger|0\rangle$, which means spontaneous Z_2^f symmetry breaking. Thus the ground state degeneracy in the topological superconductor in the non-interacting Kitaev chain model is associated with the spontaneous Z_2^f symmetry breaking as proposed by Klassen and Wen¹.

It is well known that spontaneous breaking of continuous symmetries will give rise to long range orders and gapless Goldstone modes. These long range orders are described by long range correlation functions of local operators. So that it is natural to raise the question what kind of long range (topological) order will appear in such a topological system with spontaneous broken Z_2^f symmetry. To answer this question, we define the following single-particle correlation function at two sites j and l ,

$$G_{jl} = \langle i\lambda_j^1 \lambda_l^2 \rangle, \quad (16a)$$

where the imaginary i is introduced to make G_{jl} Hermitian. Especially, the edge component of G_{jl} is given when $j = 1$ and $l = L$,

$$G_{1L} = \langle i\lambda_1^1 \lambda_L^2 \rangle. \quad (16b)$$

Note that the correlation function G_{jl} is a block of single-particle(hole) density of matrix, which can be generalized

to interacting systems and reflects the site-distribution of single-particle component in a many-particle wavefunction. As long as the bulk is uniform, the finite value of G_{1L} in the thermodynamic limit reflects the existence of edge modes.

The edge correlation function G_{1L} is easy to calculate in the case of $\Delta = t$ and $U = 0$, and is given for the ground state $|0\rangle$ by

$$G_{1L} = \langle 0 | i\lambda_1^1 \lambda_L^2 | 0 \rangle = -\sum_k U_{1k} V_{Lk}. \quad (17)$$

When $\mu \geq 2t$,

$$G_{1L} = \langle 0 | i\lambda_1^1 \lambda_L^2 | 0 \rangle = -\sum_k A_k^2 \delta_k \sin^2 kL. \quad (18)$$

As proved by Lieb et al.⁶⁹, this summation is of order of $O(1/L)$. When $\mu < 2t$,

$$\begin{aligned} G_{1L} &= \langle 0 | i\lambda_1^1 \lambda_L^2 | 0 \rangle = -U_{1k_0} V_{Lk_0} - \sum_k U_{1k} V_{Lk} \\ &= -A_{k_0}^2 \sinh^2 vL - \sum_k A_k^2 \delta_k \sin^2 kL \\ &= -\left[1 - \left(\frac{\mu}{2t}\right)^2\right] + O(1/L). \end{aligned} \quad (19)$$

The nonvanishing value of G_{1L} for $\mu < 2t$ in the thermodynamic limit reflects the topological order in the topological superconductor state. In this topological phase, we can also calculate edge correlation function G_{1L} for the topological degenerate state $|1\rangle$.

$$\begin{aligned} G_{1L} &= \langle 1 | i\lambda_1^1 \lambda_L^2 | 1 \rangle = U_{1k_0} V_{Lk_0} - \sum_k U_{1k} V_{Lk} \\ &= A_{k_0}^2 \sinh^2 vL - \sum_k A_k^2 \delta_k \sin^2 kL \\ &= \left[1 - \left(\frac{\mu}{2t}\right)^2\right] + O(1/L). \end{aligned} \quad (20)$$

Thus, for a generic ground state $|GS\rangle$, the edge correlation function in the thermodynamic limit is given by

$$\lim_{L \rightarrow \infty} G_{1L} \propto \begin{cases} 1 - \left(\frac{\mu}{2t}\right)^2, & \mu < 2t, \\ 0, & \mu \geq 2t. \end{cases} \quad (21)$$

Note that the nonzero contribution $U_{1k_0} V_{Lk_0}$ comes from the Majorana zero mode k_0 . Other modes mainly distribute in the bulk and the contributions to G_{1L} is of order of $O(1/L)$, which is neglectable in the thermodynamic limit. At the quantum critical point $\mu = 2t$, we have $v = 0$ and the wave vector of the Majorana zero mode becomes real $k_0 = \pi$. The k_0 -mode is no longer localized at edges but merges into the bulk, resulting in vanishing edge correlation function G_{1L} . In the quantum critical region,

$$G_{1L} \propto (2t - \mu)^z, \quad (22)$$

with critical exponent $z = 1$.

Now we would like to examine the behavior of G_{ij} inside the bulk, which can be done numerically. Two topologically distinct examples are investigated and shown in Fig. 2 and Fig. 3 respectively. The first example is given by $\Delta = t, \mu = 3t, U = 0$, which is in the topologically trivial phase, where a peak appears at short range with $i \sim j$ while long range correlation is absent. The second example is given by $\Delta = t, \mu = t, U = 0$, which is in the nontrivial topological superconductor phase. There exhibits a long range peak at $i = 1$ and $j = L$, and long range correlation is still absent inside the bulk.

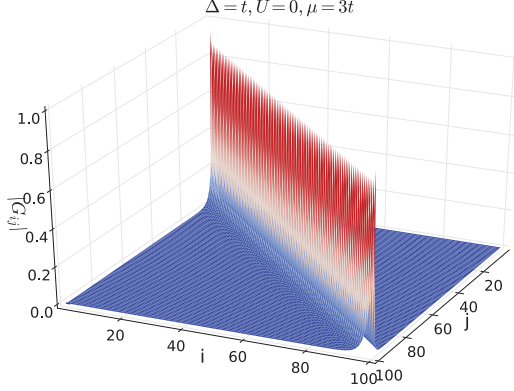


FIG. 2. Correlation function $|G_{ij}|$ for a topologically trivial state, $\Delta = t, \mu = 3t, U = 0$.

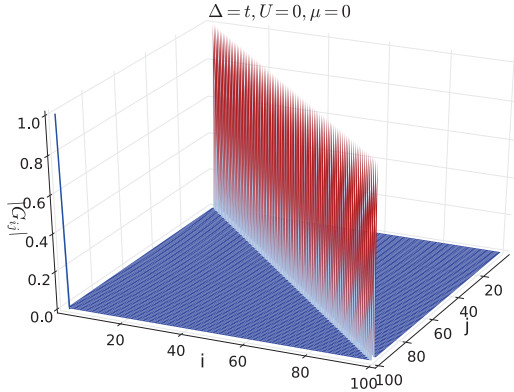


FIG. 3. Correlation function $|G_{ij}|$ for a topologically non-trivial state, $\Delta = t, \mu = 0, U = 0$.

Therefore, we propose to use the edge correlation function G_{1L} to characterize the topological order and emerged edge states. We shall examine this for the non-interacting systems with different parameters in the next subsection and for the interacting systems in the next section.

III.2. Non-interacting chains with $\mu = 0$

In this subsection, we utilize non-interacting Kitaev chains with $\mu = 0$ to study how topological order will vanish as the superconducting gap Δ approaches zero. The Hamiltonian now reads

$$H_{\Delta} = \frac{i}{2} \sum_{j=1}^{L-1} [-(t + \Delta) \lambda_{j+1}^1 \lambda_j^2 - (t - \Delta) \lambda_j^1 \lambda_{j+1}^2]. \quad (23)$$

We are able to diagonalize the Hamiltonian H_{Δ} by SVD as before. There exist two kinds of modes in this situation. For the first kind of modes, the two orthogonal matrices U and V are found to be

$$U_{jk^I} = \begin{cases} 0, & j = \text{odd}, \\ A_{k^I} \sin k^I j, & j = \text{even}, \end{cases} \quad (24a)$$

$$V_{jk^I} = \begin{cases} -A_{k^I} \delta_{k^I} \sin k^I (L + 1 - j), & j = \text{odd}, \\ 0, & j = \text{even}. \end{cases} \quad (24b)$$

The second kind of modes is given by

$$U_{jk^{II}} = \begin{cases} A_{k^{II}} \sin k^{II} (L + 1 - j), & j = \text{odd}, \\ 0, & j = \text{even}, \end{cases} \quad (25a)$$

$$V_{jk^{II}} = \begin{cases} 0, & j = \text{odd}, \\ -A_{k^{II}} \delta_{k^{II}} \sin k^{II} j, & j = \text{even}. \end{cases} \quad (25b)$$

Here the normalization factors are given by

$$A_k = 2 \left[L + 1 - \frac{\sin 2k (L + 1)}{\sin 2k} \right]^{-1/2}, \quad (26)$$

and

$$\delta_k = \text{sgn} \left[\frac{\cos k}{\cos k (L + 1)} \right]. \quad (27)$$

Corresponding singular values are given by

$$\Lambda_k = \sqrt{(2t \cos k)^2 + (2\Delta \sin k)^2}. \quad (28)$$

The wave vector k^I 's are given by the following equation,

$$\frac{\sin k^I (L + 2)}{\sin k^I L} = -\frac{t - \Delta}{t + \Delta}, \quad (29)$$

and k^{II} 's are determined by

$$\frac{\sin k^{II} (L + 2)}{\sin k^{II} L} = -\frac{t + \Delta}{t - \Delta}. \quad (30)$$

Besides $L - 1$ real k^{II} 's, there exists a single complex k^{II} in the second kind modes,

$$k_0^{II} = \frac{\pi}{2} + iv, \quad (31)$$

with v determined by

$$\frac{\sinh v (L + 2)}{\sinh v L} = \frac{t + \Delta}{t - \Delta}. \quad (32)$$

For this k_0^{II} mode we have

$$U_{jk_0^{II}} = \begin{cases} A_{k_0^{II}} (-1)^{\frac{L+1-j}{2}} \sinh v (L+1-j) & j = \text{odd}, \\ 0 & j = \text{even}, \end{cases} \quad (33a)$$

$$V_{jk_0^{II}} = \begin{cases} 0 & j = \text{odd}, \\ -A_{k_0^{II}} (-1)^{-\frac{L-j}{2}} \sinh v j & j = \text{even}. \end{cases} \quad (33b)$$

Then the normalization factor can be written explicitly,

$$A_{k_0^{II}} = 2e^{-vL} (1 - e^{-4v})^{1/2}, \quad (34)$$

and the singular value reads

$$\Lambda_{k_0^{II}} = \frac{2\Delta}{t + \Delta} \left(\frac{t - \Delta}{t + \Delta} \right)^{L/2}. \quad (35)$$

It is easy to see that the singular value of k_0^{II} mode vanishes in the thermodynamic limit,

$$\lim_{L \rightarrow \infty} \Lambda_{k_0^{II}} = 0. \quad (36)$$

The (single particle) wavefunction of this zero mode is given by

$$\begin{aligned} \langle 0 | c_j c_{k_0^{II}}^\dagger | 0 \rangle &= \frac{1}{2} (U_{jk_0^{II}} + V_{jk_0^{II}}) \\ &= \frac{A_{k_0^{II}}}{2} \begin{cases} (-1)^{\frac{L+1-j}{2}} \sinh v (L+1-j), & j = \text{odd}, \\ -(-1)^{-\frac{L-j}{2}} \sinh v j, & j = \text{even}, \end{cases} \end{aligned} \quad (37)$$

which has nonzero value only near the edge in the thermodynamic limit. Similarly, one can verify that $c_{k_0^{II}}^\dagger = \pm c_{k_0^{II}}$ at edges. Hence the k_0^{II} -mode is the Majorana zero mode localized at edges. When $\Delta \rightarrow 0$, the wave vector of the zero mode becomes real $k_0^{II} = \frac{\pi}{2}$ and the Majorana zero mode is no longer localized at edges. This is consistent with the condition for the boundary Majorana fermion argued by Kitaev⁸, i.e. the presence of an arbitrary small superconducting gap Δ .

Now we compute the edge correlation function G_{1L} for the ground state $|0\rangle$,

$$\begin{aligned} G_{1L} &= \langle 0 | i\lambda_1^\dagger \lambda_L^2 | 0 \rangle = -U_{1k_0^{II}} V_{Lk_0^{II}} - \sum_k U_{1k} V_{Lk} \\ &= (-1)^{L/2} A_{k_0^{II}}^2 \sinh^2 v L + \sum_k A_k^2 \delta_k \sin^2 k L \\ &= (-1)^{L/2} \left[1 - \left(\frac{t - \Delta}{t + \Delta} \right)^2 \right] + O(1/L), \end{aligned} \quad (38)$$

and for the topological degenerate state $|1\rangle = c_{k_0^{II}}^\dagger |0\rangle$,

$$\begin{aligned} G_{1L} &= \langle 1 | i\lambda_1^\dagger \lambda_L^2 | 1 \rangle = U_{1k_0^{II}} V_{Lk_0^{II}} - \sum_k U_{1k} V_{Lk} \\ &= -(-1)^{L/2} A_{k_0^{II}}^2 \sinh^2 v L + \sum_k A_k^2 \delta_k \sin^2 k L \\ &= -(-1)^{L/2} \left[1 - \left(\frac{t - \Delta}{t + \Delta} \right)^2 \right] + O(1/L). \end{aligned} \quad (39)$$

For small but finite Δ , we have

$$G_{1L} \propto \Delta^z, \quad (40)$$

with critical exponent $z = 1$. When $\Delta = 0$, not only the fermion number parity but also the total fermion number is conserved. The discrete Z_2^f symmetry is enlarged to the continuous U_1^f symmetry,

$$U_1^f = e^{i\theta \sum_j n_j}, \quad (41)$$

where θ can be arbitrary value in $[0, 2\pi)$ besides π . The Mermin-Wagner-Hohenberg theorem tells us that the continuous symmetry can not be spontaneous broken in one dimension^{73–75}. Thus the system does not have spontaneous symmetry breaking and does not survive any long range order.

IV. INTERACTING KITAEV CHAINS: DMRG ANALYSIS

In this section, we shall study interacting Kitaev chains by carrying out DMRG calculations in the language of matrix product states⁷⁸ with various model parameters in Hamiltonian (1) and system size up to $L = 140$. We compute the energy of low lying states, local particle density, as well as the single-particle correlation function G_{ij} .

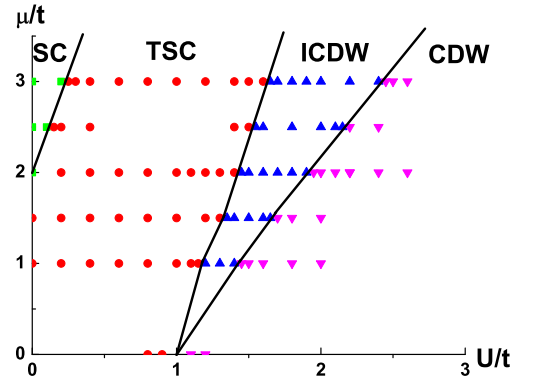


FIG. 4. Phase diagram for the interacting Kitaev chain with $\Delta = t$. SC stands for trivial superconductor, TSC stands for topological superconductor, CDW stands for charge density wave, and ICDW stands for incommensurate charge density wave. Data points are obtained within DMRG for different system sizes. Squares denote SC states, circles denote TSC states, up-triangles denote ICDW states, and down-triangles denote CDW states.

Phase diagrams. Fig. 4 displays the phase diagram at $\Delta = t$ obtained from the combination of exact solutions and DMRG calculations. As a function of μ and U , there are four distinct phases, trivial superconductor (SC), topological superconductor (TSC), commensurate

charge density wave (CDW) and incommensurate charge density wave (ICDW). The four different phases are separated from each other by critical lines. Such a phase diagram is consistent with previous studies^{39–41}.

The TSC phase is detected by the two-fold degenerate ground states with opposite fermion number parity Z_2^f . In contrast, the two ground states of CDW and ICDW phase have the same Z_2^f . In practice, we compute the matrix elements for Z_2^f in the subspace spanned by the two lowest lying states, $|0\rangle$ and $|1\rangle$, and diagonalize the 2×2 matrix to obtain two eigenvalues. The distinction between ICDW and CDW can be made through local particle density and its Fourier transformation. For a CDW state, there exists a single peak at $Q = \pi$, while for a ICDW state, there appear two peaks in the Fourier spectrum.

When $\mu = 0$, as U increases, the ground state changes from TSC to CDW directly via the critical point $U = t$. When $0 < \mu < 2t$, as U increase, the ground state changes from TSC to ICDW and to CDW in the large U limit. When $\mu > 2t$, the ground state starts with a SC state, as U increases, it changes to TSC, ICDW and to CDW finally.

Excited energy for low lying states. We compute low lying states and study the evolution of their excited energy as U increasing. The excited energy for the first and second excited states, Λ_1 and Λ_2 , are demonstrated in Fig. 5, 6, 7, and 8 for fixed $\mu = t, 1.5t, 2t$, and $3t$ respectively.

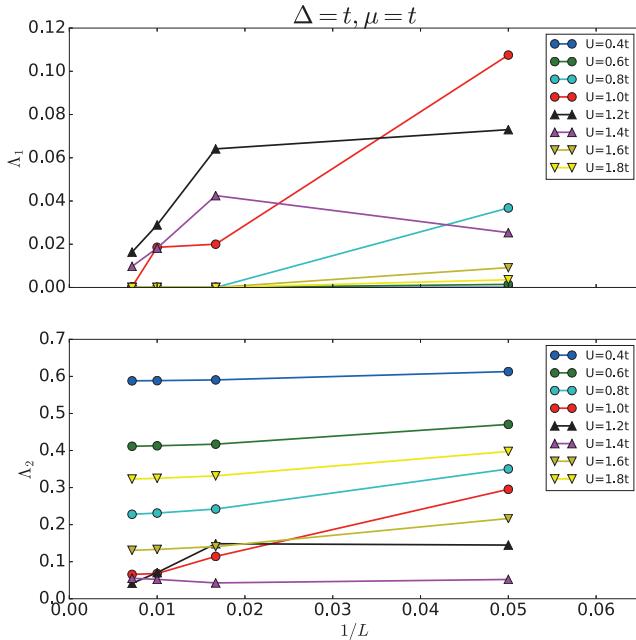


FIG. 5. Excited energy for the first and second excited states, $\mu = t$. Circles denote TSC states, up-triangles denote ICDW states, and down-triangles denote CDW states.

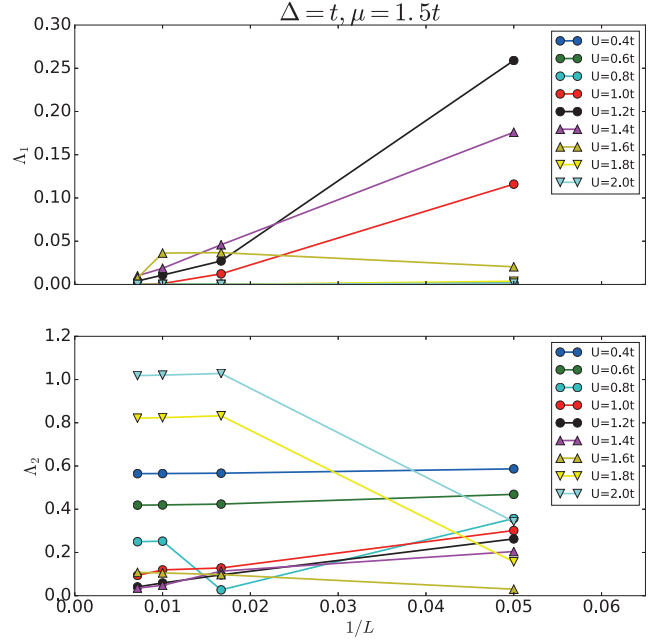


FIG. 6. Excited energy for the first and second excited states, $\mu = 1.5t$. Circles denote TSC states, up-triangles denote ICDW states, and down-triangles denote CDW states.

Single-particle correlation function G_{ij} . We also compute the single-particle correlation function G_{ij} defined in Eq. (16) for ground states. Similar to exactly solvable systems shown in Fig. 2 and Fig. 3, long range correlation is absent inside the bulk. When the system is in the TSC phase, there exists a single long range peak at $i = 1$ and $j = L$. Fig. 9 and Fig. 10 demonstrate two TSC states with $\Delta = t, \mu = 0, U = 0.5t$ and $\Delta = t, \mu = t, U = 0.5t$ respectively. So that G_{ij} serves an efficient measurement for edge states and thereby the topological order.

Edge correlation function G_{1L} . The nonvanishing edge correlation function G_{1L} characterizes the topological order. We fix $\Delta = t$ and study G_{1L} as a function of μ and U . The result is plotted in Fig. 11. The value of G_{1L} is finite in TSC phase and vanishes in other topologically trivial phases.

V. CONCLUSION

In summary, we have studied in this paper the Kitaev chains with open boundary condition by using analytic exact solution method for the non-interacting model and by using DMRG method for the interacting model. Firstly, we examine the idea proposed by Klassen and Wen¹ that the emergence of Majorana zero mode is associated with the spontaneous symmetry breaking of fermion number parity Z_2^f .

Then we study a locally defined single-particle correlation function G_{ij} and find that there exists a long-range edge correlation G_{1L} in the topologically nontrivial phase

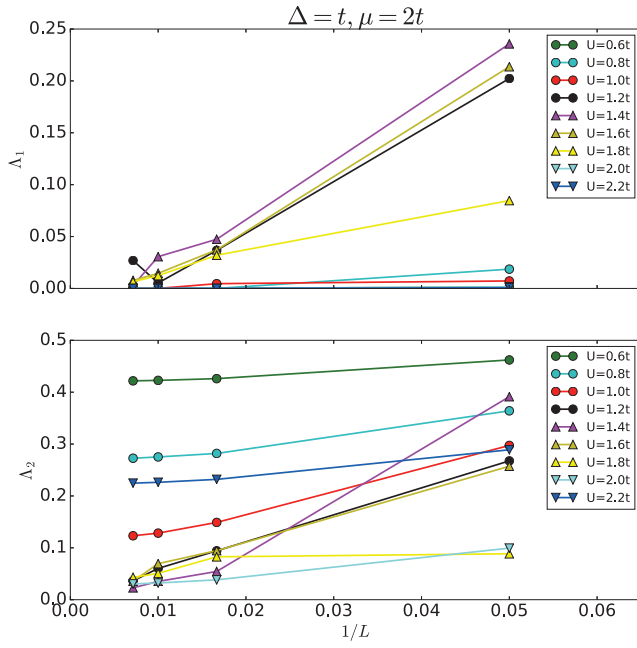


FIG. 7. Excited energy for the first and second excited states, $\mu = 2t$. Circles denote TSC states, up-triangles denote ICDW states, and down-triangles denote CDW states.

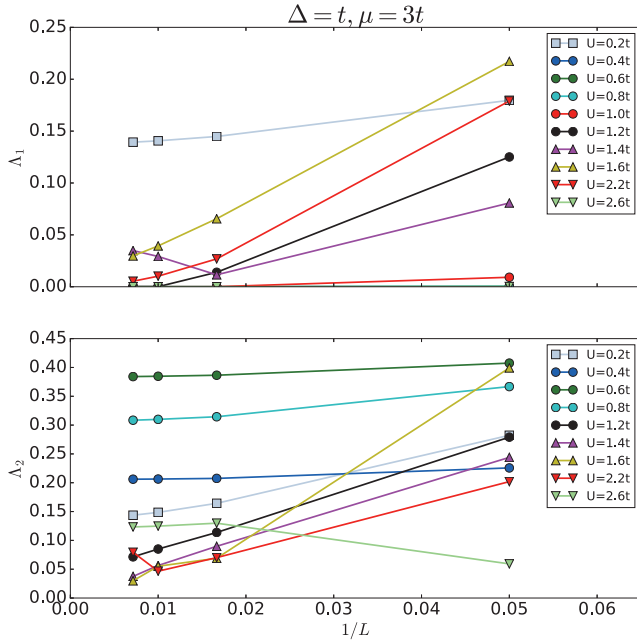


FIG. 8. Excited energy for the first and second excited states, $\mu = 3t$. Squares denote SC states, circles denote TSC states, up-triangles denote ICDW states, and down-triangles denote CDW states.

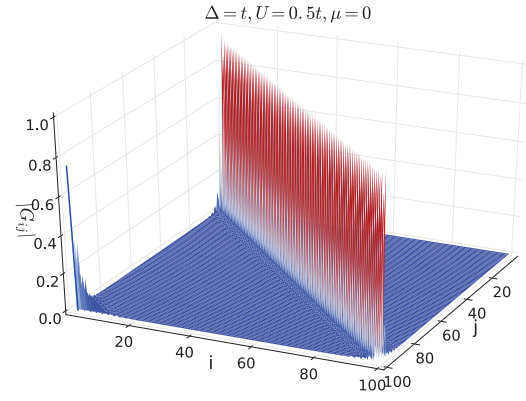


FIG. 9. Single-particle correlation function G_{ij} for the TSC ground state with $\Delta = t$, $\mu = 0$ and $U = 0.5t$. The system size is $L = 100$.

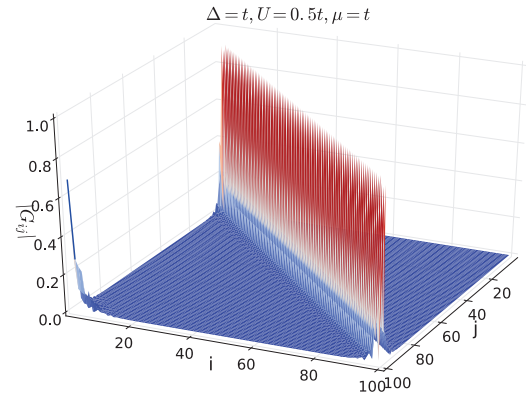


FIG. 10. Single-particle correlation function G_{ij} for the TSC ground state with $\Delta = t$, $\mu = t$ and $U = 0.5t$. The system size is $L = 100$.

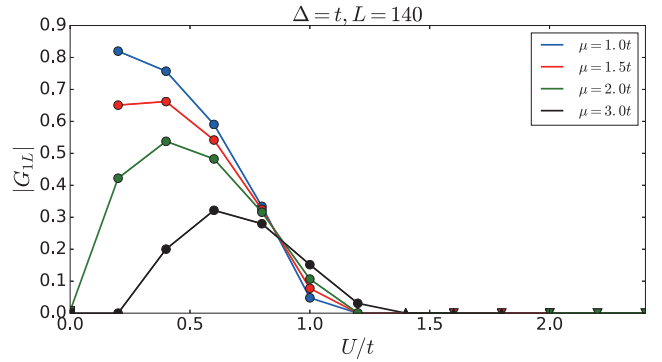


FIG. 11. Ground state edge correlation function G_{1L} as function of μ and U . $\Delta = t$ and the system size is $L = 140$. Squares denote SC states, circles denote TSC states, up-triangles denote ICDW states, and down-triangles denote CDW states.

which is absent in topologically trivial phases, while long range correlation is always absent inside bulk for all the phases. Thus, we propose that G_{1L} can be used to characterize the topological order in 1+1D fermionic systems and use it to describe quantum phase transitions between topologically trivial and nontrivial phases. It is found that $G_{1L} \propto w^z$ with $z = 1$ near the critical point, where $w = \Delta, \mu_c - \mu$, etc. is a control parameter that drives the system from a topologically nontrivial phase to a topologically trivial phase.

VI. ACKNOWLEDGEMENT

We would like to thank Xiao-Gang Wen for helpful communications, and thank Chih-Chieh Chen for his help in DMRG programming. This work is supported in part by National Basic Research Program of China (No.2014CB921201/2014CB921203), National Key R&D Program of the MOST of China (No.2016YFA0300202), NSFC (No.11374256/11274269/11674278) and the Fundamental Research Funds for the Central Universities in China. F.C.Z was also supported by the Hong Kongs University Grant Council via Grant No. AoE/P-04/08.

Appendix A: Exact diagonalization of non-interacting Kitaev chains with $\Delta = t$

In this appendix, we provide details in exact diagonalization of the matrix B in Eq. (8). We write the matrix B in the SVD form³⁹,

$$B = U\Lambda V^T, \quad (\text{A1})$$

where the matrix $\Lambda = \Lambda_k$ is diagonal. The matrices U and V are orthogonal transformations

$$\lambda_k^1 = \sum_{j=1}^L U_{jk} \lambda_j^1, \quad (\text{A2a})$$

$$\lambda_k^2 = \sum_{j=1}^L V_{jk} \lambda_j^2, \quad (\text{A2b})$$

which satisfy $UU^T = VV^T = \mathbf{1}$ and keep the anticommutation relations of the Majorana fermion operators

$$(\lambda_k^a)^\dagger = \lambda_k^a, \quad (\text{A3})$$

$$\{\lambda_k^a, \lambda_q^b\} = 2\delta_{ab}\delta_{kq}. \quad (\text{A4})$$

The energy spectra of the Hamiltonian H_μ are given by the singular values of the matrix B . We note the orthogonal matrices U and V diagonalize BB^T and B^TB , respectively

$$U^T BB^T U = \Lambda^2, \quad (\text{A5a})$$

$$V^T B^T B V = \Lambda^2. \quad (\text{A5b})$$

The singular values Λ_k are the non-negative square roots of the eigenvalues of BB^T . Similar diagonalization was found by Lieb et al. in the study of Heisenberg-Ising model⁶⁹. The orthogonal matrices U and V are found to be

$$U_{jk} = A_k \sin k(L+1-j), \quad (\text{A6a})$$

$$V_{jk} = A_k \delta_k \sin kj, \quad (\text{A6b})$$

where the normalization constant is

$$A_k = 2 \left[2L+1 - \frac{\sin k(2L+1)}{\sin k} \right]^{-1/2}, \quad (\text{A7})$$

and

$$\delta_k = \text{sgn} \left(\frac{\sin k}{\sin kL} \right), \quad (\text{A8})$$

where sgn denotes the sign function. The singular values are

$$\Lambda_k = \sqrt{(\mu + 2t \cos k)^2 + (2t \sin k)^2}. \quad (\text{A9})$$

The k 's are the roots of

$$\frac{\sin k(L+1)}{\sin kL} = -\frac{2t}{\mu}. \quad (\text{A10})$$

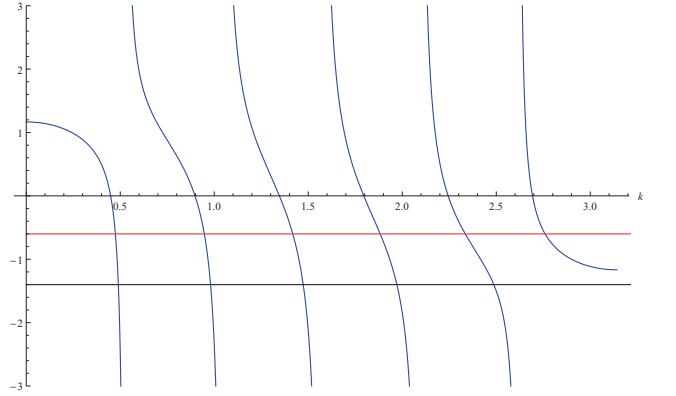


FIG. 12. $\sin k(L+1)/\sin kL$ for $L = 6$ (blue), $-2t/\mu = -0.6$ (red), $-2t/\mu = -1.4$ (black)

The graphical solution is shown in the Fig. 12. For $\mu \geq 2t$, there are L real roots, including all the normal modes. For $\mu < 2t$, there are $L-1$ real roots and one complex root

$$k_0 = \pi + iv, \quad (\text{A11})$$

with v determined by

$$\frac{\sinh v(L+1)}{\sinh vL} = \frac{2t}{\mu}. \quad (\text{A12})$$

We consider a large open chain, i.e. $vL \gg 1$

$$e^v \simeq \frac{2t}{\mu} - \left(\frac{2t}{\mu} - \frac{\mu}{2t} \right) \left(\frac{\mu}{2t} \right)^{2L}. \quad (\text{A13})$$

Then for this special mode we have

$$U_{jk_0} = A_{k_0} \sinh v (L + 1 - j), \quad (\text{A14a})$$

$$V_{jk_0} = A_{k_0} \sinh v j, \quad (\text{A14b})$$

the normalization constant becomes

$$A_{k_0} = 2e^{-vL} (1 - e^{-2v})^{1/2}, \quad (\text{A15})$$

and the singular value is

$$\Lambda_{k_0} = \left(\frac{2t}{\mu} - \frac{\mu}{2t} \right) \left(\frac{\mu}{2t} \right)^L. \quad (\text{A16})$$

Appendix B: ICDW and CDW

We can distinguish the ICDW and CDW phases by observing their local density distribution and corresponding Fourier spectrum. When the ground state is a CDW, its Fourier spectrum will have a single peak at $Q = \pi$; while for a ICDW state there are two peaks.

For various model parameters, we use the DMRG method to obtain the ground state $|0\rangle$ and local density $\langle 0 | \hat{n}_j | 0 \rangle$ for each site j . The Fourier spectrum is obtained by taking fast Fourier transformation of the local density distribution, whose average value has been subtracted. Here we show two typical figures of ICDW and CDW.

-
- ¹ J. Klassen, and X. G. Wen, J. Phys. Condens. Matter 27, 405601 (2015).
 - ² E. Majorana, Nuovo Cimento 14, 171 (1937).
 - ³ F. Wilczek, Nat. Phys. 5, 614 (2009).
 - ⁴ C. W. J. Beenakker, Annu. Rev. Condens. Matter Phys. 4, 113 (2013).
 - ⁵ S. R. Elliott and M. Franz, Rev. Mod. Phys. 87, 137 (2015).
 - ⁶ C. Nayak, S. H. Simon, A. Stern, M. Freedman, and S. Das Sarma, Rev. Mod. Phys. 80, 1083 (2008).
 - ⁷ J. Alicea, Rep. Prog. Phys. 75, 076501 (2012).
 - ⁸ A. Yu. Kitaev, Phys. Usp. 44, 131 (2001).
 - ⁹ S. Das Sarma, C. Nayak, and S. Tewari, Phys. Rev. B 73, 220502 (2006).
 - ¹⁰ G. Moore and N. Read, Nucl. Phys. B360, 362 (1991).
 - ¹¹ L. Fu and C. L. Kane, Phys. Rev. Lett. 100, 096407 (2008).
 - ¹² Y. Oreg, G. Refael, and F. von Oppen, Phys. Rev. Lett. 105, 177002 (2010).
 - ¹³ R. M. Lutchyn, J. D. Sau, and S. Das Sarma, Phys. Rev. Lett. 105, 077001 (2010).
 - ¹⁴ J. D. Sau, R. M. Lutchyn, S. Tewari, and S. Das Sarma, Phys. Rev. Lett. 104, 040502 (2010).
 - ¹⁵ S. Tewari, J. D. Sau, and S. D. Sarma, Annals of Physics 325, 219 (2010).
 - ¹⁶ J. Alicea, Phys. Rev. B 81, 125318 (2010).
 - ¹⁷ T.-P. Choy, J. M. Edge, A. R. Akhmerov, and C. W. J. Beenakker, Phys. Rev. B 84, 195442 (2011).
 - ¹⁸ S. Nadj-Perge, I. K. Drozdov, B. A. Bernevig, and A. Yazdani, Phys. Rev. B 88, 020407 (2013).
 - ¹⁹ V. Mourik, K. Zuo, S. M. Frolov, S. R. Plissard, E. P. A. M. Bakkers, and L. P. Kouwenhoven, Science 336, 1003 (2012).
 - ²⁰ L. P. Rokhinson, X. Liu, and J. K. Furdyna, Nat. Phys. 8, 795 (2012).
 - ²¹ A. Das, Y. Ronen, Y. Most, Y. Oreg, M. Heiblum, and H. Shtrikman, Nat. Phys. 8, 887 (2012).
 - ²² M. T. Deng, C. L. Yu, G. Y. Huang, M. Larsson, P. Caroff, and H. Q. Xu, Nano Lett. 12, 6414 (2012).
 - ²³ H. O. H. Churchill, V. Fatemi, K. Grove-Rasmussen, M. T. Deng, P. Caroff, H. Q. Xu, and C. M. Marcus, Phys. Rev. B 87, 241401 (2013).
 - ²⁴ E. J. H. Lee, X. Jiang, M. Houzet, R. Aguado, C. M. Lieber, and S. De Franceschi, Nat. Nanotechnol. 9, 79 (2014).
 - ²⁵ S. Nadj-Perge, I. K. Drozdov, J. Li, H. Chen, S. Jeon, J. Seo, A. H. MacDonald, B. A. Bernevig, and A. Yazdani, Science 346, 602 (2014).
 - ²⁶ M.-X. Wang et al., Science 336, 52 (2012).
 - ²⁷ J. P. Xu, M. X. Wang, Z. L. Liu, J. F. Ge, X. Yang, C. Liu, Z. A. Xu, D. Guan, C. L. Gao, D. Qian, Y. Liu, Q. H. Wang, F. C. Zhang, Q. K. Xue, and J. F. Jia, Phys. Rev. Lett. 114, 017001 (2015).
 - ²⁸ H. H. Sun, K. W. Zhang, L. H. Hu, C. Li, G. Y. Wang, H. Y. Ma, Z. A. Xu, C. L. Gao, D. D. Guan, Y. Y. Li, C. Liu, D. Qian, Y. Zhou, L. Fu, S. C. Li, F. C. Zhang, and J. F. Jia, Phys. Rev. Lett. 116, 257003 (2016).
 - ²⁹ T. Giamarchi, *Quantum Physics in One Dimension* (Oxford University Press, Oxford, 2003).
 - ³⁰ A. P. Schnyder, S. Ryu, A. Furusaki and A. W. W. Ludwig, Phys. Rev. B 78 195125 (2008).
 - ³¹ A. P. Schnyder, S. Ryu, A. Furusaki and A. W. W. Ludwig, New J. Phys. 12 065010 (2010).
 - ³² A. Y. Kitaev, AIP Conf. Proc. 1134 22 (2009).
 - ³³ L. Fidkowski and A. Kitaev, Phys. Rev. B 81, 134509 (2010).
 - ³⁴ X. G. Wen, Phys. Rev. B 40, 7387 (1989).
 - ³⁵ X. G. Wen and Q. Niu, Phys. Rev. B 41, 9377 (1990).
 - ³⁶ X. G. Wen, Int. J. Mod. Phys. B 4, 239 (1990).
 - ³⁷ E. Keski-Vakkuri and X. G. Wen, Int. J. Mod. Phys. B 7, 4227 (1993).
 - ³⁸ X. G. Wen, *Quantum Field Theory of Many-body Systems From the Origin of Sound to an Origin of Light and Electrons* (Oxford University Press, Oxford, 2004).
 - ³⁹ H. Katsura, D. Schuricht and M. Takahashi, Phys. Rev. B 92, 115137 (2015).
 - ⁴⁰ Armin Rahmani, Xiaoyu Zhu, Marcel Franz, and Ian Aflleck, Phys. Rev. B 92, 235123 (2015).
 - ⁴¹ Ronny Thomale, Stephan Rachel, and Peter Schmitteckert, Phys. Rev. B 88, 161103(R) (2013).
 - ⁴² Niklas M. Gergs, Lars Fritz, and Dirk Schuricht Phys. Rev. B 93, 075129 (2016).
 - ⁴³ S. Gangadharaiah, B. Braunecker, P. Simon, and D. Loss, Phys. Rev. Lett. 107, 036801 (2011).
 - ⁴⁴ E. M. Stoudenmire, J. Alicea, O. A. Starykh, and M. P. A. Fisher, Phys. Rev. B 84, 014503 (2011).
 - ⁴⁵ R. Thomale, S. Rachel, and P. Schmitteckert, Phys. Rev. B 88, 161103 (2013).
 - ⁴⁶ A. Manolescu, D. C. Marinescu, and T. D. Stanescu, J. Phys. Condens. Matter 26, 172203 (2014).
 - ⁴⁷ Y. H. Chan, C. K. Chiu, and K. Sun, Phys. Rev. B 92, 104514 (2015).

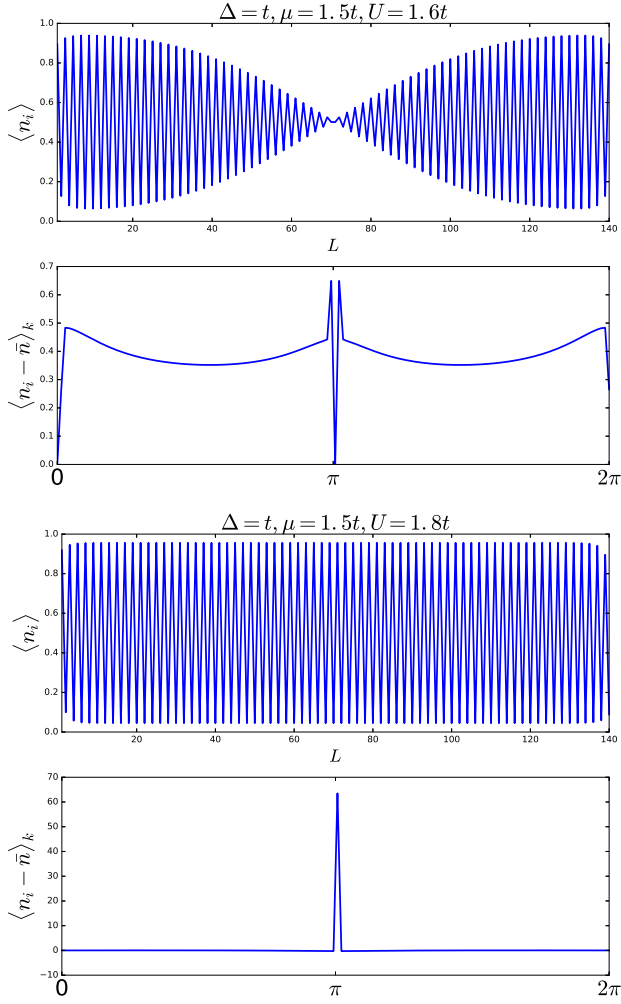


FIG. 13. Local density distribution and density spectrum. In up figure the local density of ICDW oscillates nonuniformly and its Fourier spectrum has two peaks near $Q = \pi$. In bottom figure the local density of CDW forms a bipartite lattice and the Fourier spectrum has single peaks at $Q = \pi$.

- ⁴⁸ R. M. Lutchyn and M. P. A. Fisher, Phys. Rev. B 84, 214528 (2011).
⁴⁹ E. Sela, A. Altland, and A. Rosch, Phys. Rev. B 84, 085114 (2011).
⁵⁰ M. Cheng and H. H. Tu, Phys. Rev. B 84, 094503 (2011).
⁵¹ F. Hassler and D. Schuricht, New J. Phys. 14, 125018

- (2012).
⁵² C. K. Chiu, D. I. Pikulin, and M. Franz, Phys. Rev. B 91, 165402 (2015).
⁵³ A. M. Lobos, R.M. Lutchyn, and S. Das Sarma, Phys. Rev. Lett. 109, 146403 (2012).
⁵⁴ F. Crépin, G. Zaránd, and P. Simon, Phys. Rev. B 90, 121407 (2014).
⁵⁵ Fernando Iemini, Leonardo Mazza, Davide Rossini, Rosario Fazio, and Sebastian Diehl, Phys. Rev. Lett. 115, 156402(2015).
⁵⁶ L. Fidkowski and A. Kitaev, Phys. Rev. B 83, 075103 (2011).
⁵⁷ A. M. Turner, F. Pollmann, and E. Berg, Phys. Rev. B 83, 075102 (2011).
⁵⁸ G. Goldstein and C. Chamon, Phys. Rev. B 86, 115122 (2012).
⁵⁹ G. Kells, Phys. Rev. B 92, 081401 (2015).
⁶⁰ T. Grover, D. N. Sheng, and A. Vishwanath, Science 344, 280 (2014).
⁶¹ J. Ulrich, İ. Adagideli, D. Schuricht, and F. Hassler, Phys. Rev. B 90, 075408 (2014).
⁶² A. Rahmani, X. Zhu, M. Franz, and I. Affleck, Phys. Rev. Lett. 115, 166401 (2015).
⁶³ A. Rahmani, X. Zhu, M. Franz, and I. Affleck, Phys. Rev. B 92, 235123 (2015).
⁶⁴ P. Fendley, J. Stat. Mech. (2012) P11020.
⁶⁵ D. J. Clarke, J. Alicea, and K. Shtengel, Nat. Phys. 10, 877 (2014).
⁶⁶ J. Klinovaja and D. Loss, Phys. Rev. Lett. 112, 246403 (2014).
⁶⁷ A. S. Jermyn, R. S. K. Mong, J. Alicea, and P. Fendley, Phys. Rev. B 90, 165106 (2014).
⁶⁸ A. Alexandradinata, N. Regnault, C. Fang, M. J. Gilbert, and B. A. Bernevig, arXiv:1506.03455.
⁶⁹ E. Lieb, T. Schultz and D. Mattis, Ann. Phys. 16, 407 (1961).
⁷⁰ X. L. Qi and S. C. Zhang, Rev. Mod. Phys. 83, 1057 (2011).
⁷¹ B. A. Bernevig and T. L. Hughes, *Topological Insulators and Topological Superconductors* (Princeton University Press, Princeton and Oxford, 2013).
⁷² P. Pfeuty, Ann. Phys. 57, 79 (1970).
⁷³ N.D. Mermin and H. Wagner, Phys. Rev. Lett. 17, 1133C1136 (1966).
⁷⁴ P.C. Hohenberg, Phys. Rev. 158, 383 (1967).
⁷⁵ S. Coleman, Commun. Math. Phys. 31, 259 (1973).
⁷⁶ M. Oshikawa, Phys. Rev. Lett. 84, 1535 (2000).
⁷⁷ M. Oshikawa, Phys. Rev. Lett. 90, 236401 (2003).
⁷⁸ U. Schollwck, The density-matrix renormalization group in the age of matrix product states, Ann. Phys. 326, 96 (2011).